善したかどうかの印象，③The Brief Psychiatric Rating Scale(BPRS)の3項目すべてにおいて，改善もしくは悪化していない場合を「効果あり」とみなす．補助的に，画像検査(MRI)，生理学的検査(EEG)，血液学的もしくは髄液検査におけるCJDマーカーなどの客観的検査項目を評価する．われわれのキナクリン治療の効果判定では，臨床観察に重点を置き，「一過性だとしても効果があった」という結論に至った事情があるが，本試験ではその視点もとり込まれているわけである．加えて客観的な指標でも効果判定するという点では，これまでにないより多角的な評価が可能となり，期待が持てる．2005年6月3日の時点で，43例の対象が集められていることも付記しておく．福岡大学におけるキナクリン変法(シメチジン，塩酸ベラパミル併用)はいまだ症例が少なく，今後の症例の蓄積が望まれる．他の治療的試みとして，ペントサンポリサルフェートの脳室内治療が始まっているが，観血的に脳室内にチューブを留置することが必要となり，実施できる施設が限られている．刻々と病状が進行していくCJD患者に対して，内服のみで施行できるキナクリン治療を再度見直し，臨床試験の結果を踏まえて，今後さらにふさわしい治療の基礎を模索しようという意図は評価してもよいであろう．

まとめ

Creutzfeldt-Jakob病に対するキナクリン・キニーネ治療について，これまでの治療経過と，今後の展望について述べた．一過性の効果，もしくは効果がないとみなされていた同治療であるが，抗プリオン作用があり，ヒトに比較的安全に使えると予想される薬物は，現時点においてキナクリンやペントサンポリサルフェートなどに限られているため，イギリスでは2004年6月からキナクリンを用いた新たな臨床試験が始まっている．さらなる症例の集積とともに，より臨床効果を有し，安全に投与できる抗プリオン物質の発見を期待したい．

文　献

1) Bolton DC, McKinley MP, Prusiner SB. Identification of a protein that purifies with the scrapie prion. Science 1982 ; 218 : 1309-10.
2) Korth C, May BC, Cohen FE, et al. Acridine and phenothiazine derivatives as pharmacotherapeutics for prion disease. Proc Natl Acad Sci USA 2001 ; 98 : 9836-41.
3) Doh-Ura K, Iwaki T, Caughey B. Lysosomototropic agents and cyteine protease inhibitors inhibit scrapie-associated prion protein accumulation. J Virol 2000 ; 74 : 4894-7.
4) 厚生労働省・即戦力クロイツフェルト・ヤコブ病治療法の確立に関する研究班「クロイツフェルト・ヤコブ病患者におけるキナクリン治療の効果と安全性に関する報告書」(主任研究者　堂浦克美)．東京：厚生労働省；2003年1月．
5) Haik S, Brandel JP, Salomon D,et al. Compassionate use of quinacrine in Creutzfeldt-Jakob disease fails to show significant effects. Neurology 2004 ; 63 : 2413-15.
6) Collins SJ, Lewis V, Brazier M, et al. Quinacrine does not prolong survival in a murine Creutzfeldt-Jakob disease model. Ann Neurol 2002 ; 52 : 503-6.
7) Barret A, Tagliavini F, Forloni G, et al. Evaluation of quinacrine treatment for prion diseases. J Virol 2003 ; 77 : 8462-9.
8) PRION-1 : Randomised trial of quinacrine in human prion disease ; http://www.ctu.mrc.ac.uk/studies/cjd.asp

*　　*　　*

Cellular and Molecular Neurobiology, Vol. 25, No. 5, August 2005 (©2005)
DOI: 10.1007/s10571-005-4956-5

Short Communication

Cyclosporin A Aggravates Electroshock-Induced Convulsions in Mice with a Transient Middle Cerebral Artery Occlusion

Atsushi Yamauchi,[1] Hideki Shuto,[1] Shinya Dohgu,[1] Yoshitsugu Nakano,[1] Takashi Egawa,[1] and Yasufumi Kataoka[1,2]

Received January 11, 2005; accepted February 18, 2005

SUMMARY

1. To test whether an ischemic insult increases the susceptibility to cyclosporine A (CsA)-induced neurotoxicity, we examined the effect of CsA on the minimal electroshock-induced convulsions in mice treated with a transient middle cerebral artery occlusion (MCAO) for a short period (2 h).

2. This MCAO produced small to mid-sized infarcted regions in the cerebral hemisphere with increasing post-operative days. In MCAO mice, CsA (30 mg/kg, i.p.) elevated the incidence of minimal electroshock-induced convulsions to 90–100% over that in sham mice (20–30%) at 1–7 days but not 14 days post-surgery.

3. In light of these findings, the possibility that CsA increases the risk of convulsions in patients with cerebral infarction and/or at an early stage following focal cerebral ischemia would have to be considered.

KEY WORDS: cyclosporin A; electroshock-induced convulsions; middle cerebral artery occlusion; blood-brain barrier; mice.

INTRODUCTION

Cyclosporin A (CsA), an immunosuppressant, is widely used to prevent allograft rejection in solid organ transplantation and to treat various autoimmune diseases. CsA induces adverse events including renal, cardiovascular and gastrointestinal disorders. Neurological complications occur with a relatively high frequency (20–40%) (Gijitenbeek *et al.*, 1999; U. S. Group, 1994). The delivery of CsA into the brain is

[1] Department of Pharmaceutical Care and Health Sciences, Faculty of Pharmaceutical Sciences, Fukuoka University, 8-19-1 Nanakuma, Jonan-ku, Fukuoka 814-0180, Japan.
[2] To whom correspondence should be addressed; e-mail: ykataoka@cis.fukuoka-u.ac.jp.

restricted by P-glycoprotein, a multi-drug efflux pump, and the tight junctions of brain capillary endothelial cells. CsA inhibited the function and expression of P-glycoprotein (Kochi *et al.*, 1999) and increased the permeability of brain endothelial cells (Dohgu *et al.*, 2000), suggesting that CsA could pass through the blood-brain barrier (BBB) due to the impaired function. In the present study, to test whether CsA induces neurotoxicity by passing through the damaged BBB and/or the reconstituted BBB with an incomplete function after an ischemic insult, we examined the effect of CsA on minimal electroshock-induced convulsions in mice treated with a transient middle cerebral artery occlusion (MCAO) for a short period (2 h).

MATERIALS AND METHODS

Male ddY mice weighing 25–35 g (Kyudo, Kumamoto, Japan) were housed in a room at a temperature of 22 ± 2°C under a 12-h light/dark schedule (lights on at 7:00 hours) and given water and food ad libitum. All the procedures involving experimental animals adhered to the law (No. 105) and notification (No. 6) of the Japanese Government, and were approved by the Laboratory Animal Care and Use Committee of Fukuoka University.

The pharmaceutical formulation of CsA (Sandimmun® injection, 250 mg/5 mL/ampule, Novartis Pharma, Tokyo, Japan) was used after a dilution with saline. The vehicle solution for CsA consisted of 13% polyoxyethylene castor oil (Cremophor EL®, Sigma, St. Louis, MO, USA), 7% ethanol, and 80% saline (the same mixture as the vehicle for Sandimmun® injection). A reagent for histological examination, 2,3,5-triphenyltetrazolium chloride (TTC), was purchased from Sigma.

Anesthesia was induced by 2% halothane (Flosen, Takeda, Osaka, Japan) and maintained with 1% halothane. Focal cerebral ischemia was induced by occlusion of the middle cerebral artery using the intraluminal filament technique (Mishima *et al.*, 2003). After a midline neck incision, the left common and external carotid arteries were isolated and ligated. An 8-0 nylon monofilament (Ethilon, Johinson & Johinson, Tokyo, Japan) coated with silicon resin (Xantopren, Heleus Dental Material, Osaka, Japan) was introduced through a small incision into the common carotid artery and was advanced to a position 9 mm distal from the carotid bifurcation for occlusion of the middle cerebral artery. Two hours after MCAO, animals were re-anesthetized with halothane, and reperfusion was established by withdrawal of the filament. The sham-operated mice were subjected to the procedure mentioned above without MCAO. At the end of the experiment, mice were decapitated under anesthesia with pentobarbital Na (40 mg/kg, i.p., Nembutal, Dainippon, Osaka, Japan) and brains were removed. Coronal sections were cut 2-mm thick and incubated in physiological saline containing 2% TTC at 37°C for 15 min for histological examination of the MCAO-induced brain damage.

Effect of CsA or vehicle on the minimal electroshock-induced convulsions was examined at 1, 3, 7 and 14 days after the sham-operation or MCAO. CsA (10 and 30 mg/kg) or vehicle was administered i.p. in a volume of 0.1 mL/10 g body weight. Sixty minutes after the injection, each mouse was subjected to the minimal electroshock (10 mA, at a frequency of 60 Hz, applied for 0.2 s) using

external corneal electrodes connected to an electroshock convulsive stimulator unit (MK-800, Muromachi Kikai, Tokyo, Japan) and placed individually in an acrylic cage (18 × 28 × 34 cm). The observations were made during a 2-min period with a camcorder (VL-DC1, Sharp, Tokyo, Japan) and stored on digital video tape. The durations of clonic and tonic-clonic convulsions were measured with a video player by two observers blinded to the pretreatment with CsA or vehicle. The minimal electroshock-induced convulsions were defined as positive when they lasted for more than 2 s. Only one of 12 normal mice showed convulsions for 1 s.

Statistical analysis was performed using Fisher's exact probability test. A value of $P < 0.05$ was considered significant.

RESULTS

Histological observations with TTC staining indicated that MCAO for 2 h produced a small infarcted region in the caudate putamen of the cerebral hemisphere with a relatively mild insult (an irregular pallor) at 1 day after the operation (Fig. 1). The size and intensity of infarction gradually increased in the cuadate putamen and cerebral cotex at 3–7 days, reaching a maximum at 14 days. Minimal electroshock did not induce convulsions in sham mice treated with vehicle. When CsA (10 or 30 mg/kg) was given, convulsions were induced by electroshock in 20–30% of sham mice at 1–14 days post-surgery (Fig. 2A). In MCAO mice treated with vehicle, electroshock-induced convulsion was observed in 1 of 8 mice at 1 day, but not at 3–14 days post-surgery (Fig. 2B). In MCAO mice, CsA (10 mg/kg) moderately increased the incidence of convulsions to 67% over the level in sham mice (20–30%) at 1 day but not at 3–14 days after operation (Fig. 2). CsA (30 mg/kg) markedly increased the incidence of convulsions to 90–100% at 1–7 days, but this increase was not observed at 14 days after the operation in MCAO mice (Fig. 2B).

DISCUSSION

Treatment with MCAO is employed to make an animal model of transient focal cerebral ischemia (Brown *et al.*, 1995; Sydserff *et al.*, 2002). In the present study, a short (2 h) MCAO produced small to mid-sized infarcted regions with increasing post-operative days in the caudate putamen and cerebral cortex, when compared with the usual MCAO method (4 h) (Mishima *et al.*, 2003) (Fig. 1).

A high dose of CsA (30 mg/kg) markedly aggravated the electroshock-induced convulsions in MCAO mice. This action appeared at an early stage (1–7 days) but not late stage (14 days) post-MCAO. An ischemic event has been known to cause disruption of the BBB (Cipolla *et al.*, 2004). Nishigaya *et al.* demonstrated using an immunohistological staining of endothelial barrier antigen that impairment and restoration of the brain endothelial barrier occurred in the post-ischemic period of 1–7 days and 14–28 days, respectively, in rats with MCAO for 2 h. Taken together with this evidence, the present findings suggest that CsA probably penetrates the brain through the impaired BBB at an early stage following ischemic insults and consequently has an adverse central action. The reconstituted BBB at a late-stage

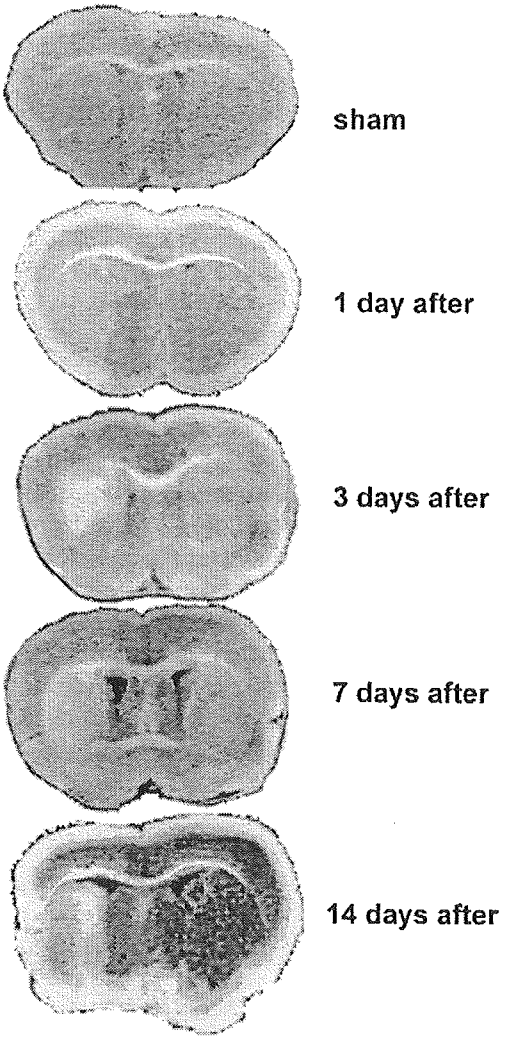

Fig. 1. Representative photographs showing coronal sections of the caudate putamen and cerebral cortex stained with 2% 2,3,5-triphenyltetrazolium chloride at 1, 3, 7 and 14 days after a transient middle cerebral artery occlusion for 2 h and at 7 days after sham operation (Sham).

post-MCAO may limit the delivery of CsA. Our previous findings *in vitro* demonstrated that CsA impairs brain endothelial barrier function by accelerating NO production in brain endothelial and astroglial cells (Ikesue *et al.*, 2000; Dohgu *et al.*, 2000; Yamauchi *et al.*, 2005). This action of CsA may be effective against the damaged BBB and/or the reconstituted BBB with an incomplete function at an early stage following the pathological insult. CsA is known to induce convulsions as a result of an

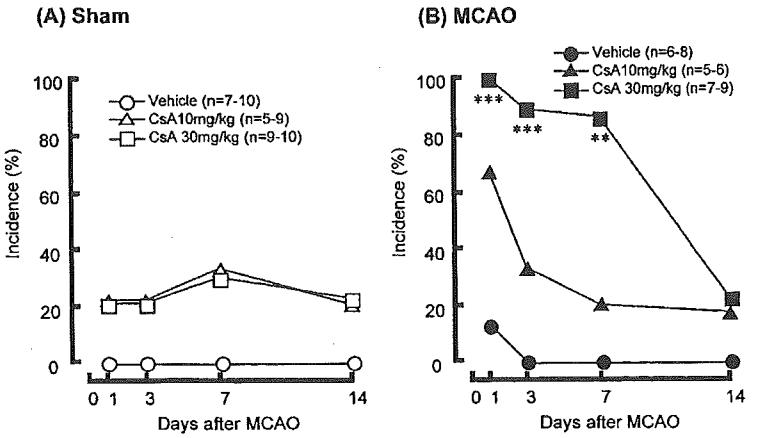

Fig. 2. Effect of cyclosporin A (CsA) on minimal electroshock-induced convulsions in sham-operated mice (Sham) (A) and in mice with a transient middle cerebral artery occlusion for 2 h (MCAO) (B). Values are expressed as the incidence (%) of convulsions in mice injected with vehicle or CsA 1 h before the test. The number of mice used in each treatment is indicated in parentheses. $^{**}P < 0.01$ and $^{***}P < 0.001$; significant difference from each corresponding group treated with vehicle.

interaction between NO and the γ-aminobutyric acid system in the hippocampus (Shuto *et al.*, 1999; Fujisaki *et al.*, 2002). This may be interpreted as a possible mechanism for the adverse central action of CsA after penetration of the brain. The possibility that MCAO influences these neuronal systems and increases the susceptibility to the deleterious effect of CsA on convulsions could not be excluded.

There is experimental evidence that CsA at low doses produces neuroprotective effects when given 30 min before or several minutes to 3 h after brain ischemia (Kuroda *et al.*, 1999; Yoshimoto *et al.*, 1999). In these studies, CsA prevented neuronal cell death including necrosis and apoptosis and decreased the infarct volumes in the brain. The different dosing schedule and doses of CsA are probably responsible for the discrepancy in the results.

In light of these findings, the possibility that CsA increases the risk of convulsions in patients with cerebral infarction and/or at an early stage following focal cerebral ischemia would have to be considered.

ACKNOWLEDGMENTS

This work was supported, in part, by Grants-in-Aid for Scientific Research ((B)(2) 14370789) and ((C)(2) 15590475) from JSPS, Japan, by a Grant-in-Aid for Exploratory Research (16659138) from MEXT, Japan, by funds (No.: 031001) from the Central Research Institute of Fukuoka University and by MEXT. HAITEKU (2000–2004).

REFERENCES

Brown, C. M., Calder, C., Linton, C., Small, C., Kenny, B. A., Spedding, M., and Patmore, L. (1995). Neuroprotective properties of lifarizine compared with those of other agents in a mouse model of focal cerebral ischaemia. *Br. J. Pharmacol.* **115**:1425–1432.

Cipolla, M. J., Crete, R., Vitullo, L., and Rix, R. D. (2004). Transcellular transport as a mechanism of blood-brain barrier disruption during stroke. *Front. Biosci.* **9**:777–785.

Dohgu, S., Kataoka, Y., Ikesue, H., Naito, M., Tsuruo, T., Oishi, R., and Sawada, Y. (2000). Involvement of glial cells in cyclosporine-increased permeability of brain endothelial cells. *Cell. Mol. Neurobiol.* **20**:781–786.

Fujisaki, Y., Yamauchi, A., Dohgu, S., Sunada, K., Yamaguchi, C., Oishi, R., and Kataoka, Y. (2002). Cyclosporine A-increased nitric oxide production in the rat dorsal hippocampus mediates convulsions. *Life Sci.* **72**:549–556.

Gijitenbeek, J. M. M., Van den Bert, M. J., and Vecht, Ch. J. (1999). Cyclosporine neurotoxicity: A review. *J. Neurol.* **246**:339–346.

Ikesue, H., Kataoka, Y., Kawachi, R., Dohgu, S., Shuto, H., and Oishi, R. (2000). Cyclosporine enhances α1-adrenoreceptor-mediated nitric oxide production in C6 glioma cells. *Eur. J. Pharmacol.* **407**:221–226.

Kochi, S., Takanaga, H., Matsuo, H., Naito, M., Tsuruo, T., and Sawada, Y. (1999). Effect of cyclosporine A or tacrolimus on the function of blood-brain barrier cells. *Eur. J. Pharmacol.* **372**:287–295.

Kuroda, S., Janelidze, S., and Siesjo, B. K. (1999). The immunosuppressants cyclosporin A and FK506 equally ameliorate brain damage due to 30-min middle cerebral artery occlusion in hyperglycemic rats. *Brain Res.* **835**:148–153.

Mishima, K., Tanaka, T., Pu, F., Egashira, N., Iwasaki, K., Hidaka, R., Matsunaga, K., Takata, J., Karube, Y., and Fujiwara, M. (2003). Vitamin E isoforms alpha-tocotrienol and gamma-tocopherol prevent cerebral infarction in mice. *Neurosci. Lett.* **337**:56–60.

Nishigaya, K., Yagi, S., Sato, T., Kanemaru, K., and Nukui, H. (2000). Impairment and restoration of the endothelial blood-brain barrier in the rat cerebral infarction model assessed by expression of endothelial barrier antigen immunoreactivity. *Acta Neuropathol.* **99**:231–237.

Shuto, H., Kataoka, Y., Fujisaki, K., Nakao, T., Sueyasu, M., Miura, I., Watanabe, Y., Fujiwara, M., and Oishi, R. (1999). Inhibition of GABA system involved in cyclosporine-induced convulsions. *Life Sci.* **65**:879–887.

Sydserff, S. G., Borelli, A. R., Green, A. R., and Cross, A. J. (2002). Effect of NXY-059 on infarct volume after transient of permanent middle cerebral artery occlusion in the rat; studies on dose, plasma concentration and therapeutic time window. *Br. J. Pharmacol.* **135**:103–112.

The U.S. Multicenter FK506 Liver Study Group (1994). A comparison of tacrolims (FK 506) and cyclosporine for immunosuppression in liver transplantation. *N. Engl. J. Med.* **331**:1110–1115.

Yamauchi, A., Dohgu, S., Naito, M., Tsuruo, T., Sawada, Y., Kai, M., and Kataoka, Y. (2005). Nitric oxide lowers the function of tight junction and P-glycoprotein at the blood-brain barrier. *Cell. Mol. Neurobiol.* in press.

Yoshimoto, T., and Siesjo, B. K. (1999). Posttreatment with the immunosuppressant cyclosporin A in transient focal ischemia. *Brain Res.* **839**:283–291.

Science Express

Reciprocal Interference Between Specific CJD and Scrapie Agents in Neural Cell Cultures

Noriuki Nishida, Shigeru Katamine, Laura Manuelidis

21 October 2005, Volume 310, pp. 493-496

Reciprocal Interference Between Specific CJD and Scrapie Agents in Neural Cell Cultures

Noriuki Nishida,[1,2] Shigeru Katamine,[3] Laura Manuelidis[1]*

Infection of mice with an attenuated Creutzfeldt-Jakob disease agent (SY-CJD) interferes with superinfection by a more virulent human-derived CJD agent (FU-CJD) and does not require pathological prion protein (PrPres). Using a rapid coculture system, we found that a neural cell line free of immune system cells similarly supported substantial CJD agent interference without PrPres. In addition, SY-CJD prevented superinfection by sheep-derived Chandler (Ch) and 22L scrapie agents. However, only 22L and not Ch prevented FU-CJD infection, even though both scrapie strains provoked abundant PrPres. This relationship between particular strains of sheep- and human-derived agents is likely to affect their prevalence and epidemic spread.

In transmissible spongiform encephalopathies (TSEs) such as human CJD, sheep scrapie, and bovine spongiform encephalopathy (BSE), B and T cell adaptive immune responses to a foreign infectious agent have not been detected (*1*). Nonetheless, an attenuated CJD agent, designated SY, was able to prevent superinfection by the more virulent and rapidly lethal FU-CJD agent (*2*). These experiments exploited two human CJD agents that, when passaged in mice, were readily distinguished by profound differences in the incubation time to disease and the distribution of brain lesions. The attenuated "slow" SY produced only small medial thalamic lesions typical of sporadic CJD in mice, whereas the virulent "fast" FU strain, isolated only in Japan, caused widespread severe lesions with many amyloid deposits (Table 1). Clear protective effects of SY-CJD against superinfection by FU-CJD were demonstrable with both intracerebral and peripheral challenges, and SY-protected mice could live free of disease for >600 days, a typical mouse life span (*3*, *4*). By comparison, there was minimal interference between scrapie strains 22C and 22A (*5*). This raised the possibility that protective effects might be restricted to particular strains of CJD or to unusual agent strain combinations. We sought ways to evaluate interference between different combinations of TSE agents, and to determine whether apparently unrelated agents—such as those propagated from human CJD and from sheep scrapie cases—could be antagonistic.

Mice can respond to CJD agents through a variety of myeloid cell and innate defense mechanisms (*6*–*8*). Thus, it was relevant to determine whether different agent strains could prevent superinfection in simplified cell cultures that lack B, T, and myeloid cells. Neural cells, which can be susceptible to TSE agents, would be incapable of producing many of the myeloid cell cytokines that can participate in strain interference in vivo. If interference could be demonstrated in neural cells, it would show that more universal cellular pathways are sufficient for protection. These culture models also might be used to identify crucial, and possibly novel, molecular pathways of innate immunity to TSE agents.

We developed a rapid, simple, and flexible test of interference in GT1-7 cells (hereafter called GT cells), a murine hypothalamic cell line. We previously found that these cells support the replication of a variety of mouse-passaged CJD and scrapie agents (Table 1) (*9*, *10*). A neomycin-resistant plasmid was introduced into the target GT cells (GTneo) to allow their selection by G418 antibiotic treatment (*11*) (Fig. 1). Infected GT challenge cells were killed by adding G418 to cocultures, and the pure GTneo target cells were then passaged and assayed for PrPres, a surrogate marker for infection in GT cells. Although PrPres does not quantitatively correlate with infectious

[1]Yale Medical School, New Haven, CT 06510, USA. [2]Center for Emerging Infectious Diseases, Gifu University, Yanagido 1-1, Gifu 501-1193, Japan. [3]Department of Molecular Microbiology and Immunology, Nagasaki University Graduate School of Medicine, 1-12-4 Sakamoto, Nagasaki 852-8523, Japan.

*To whom correspondence should be addressed. E-mail: laura.manuelidis@yale.edu

Table 1. Cell lines and TSE agents for testing interference. Agents, their source, and the number of cell passages after infection at the time of challenge are shown. By convention, TSE agent names identify the natural host. Thus, scrapie agents are derived from sheep, CJD agents from humans, CWD agents from cervids, and BSE agents from cows. Hence, the terms mouse scrapie and PrP^{Sc} (i.e., PrPres in mice infected with scrapie) indicate infection with sheep-derived agents. The UK Chandler (Ch) "drowsy" strain [equivalent to Rocky Mountain Laboratory (RML) scrapie], from a goat with experimental scrapie, is distinct from 22L scrapie (typical scratching scrapie in sheep from brain pool SSBP1). These scrapie strains are clearly different from CJD and BSE agents propagated in mice (i.e., their separate identities are not made homogeneous by the murine host). CJD encompasses all subsets of human TSE infectious agents except kuru, including those isolated from patients with PrP mutations such as PrP 102L of Gerstmann-Sträussler-Sheinker disease (GSS). SY-CJD causes circumscribed thalamic lesions only after ≥350 days in mice, and it is representative of sporadic CJD agents in the Western hemisphere, including agents isolated from GSS patients (*23*). No CJD agent similar to the representative Japanese fast FU-CJD agent ("CJD-Fukuoka-1") that induces widespread PrP amyloid deposits and severe demyelination has ever been isolated outside of Japan. Because FU-CJD and the Ch and 22L scrapie strains all cause widespread brain pathology, interference between these strains cannot be assessed in mice.

Cell line	Agent strain	Origin	Passages
GT (GT1-7)	—	—	—
SY+GT	SY	CJD sporadic: USA	≥106
FU+GT	FU	CJD (GSS 102L): Japan	≥110
Ch+GT	Ch	"Drowsy" scrapie: UK	≥50
22L+GT	22L	"Scratching" scrapie: UK	≥50
GTneo	Mock	—	≥15
SY+GTneo	SY	CJD sporadic: USA	≥110
Ch+GTneo	Ch	"Drowsy" scrapie: UK	≥15
22L+GTneo	22L	"Scratching" scrapie: UK	≥15

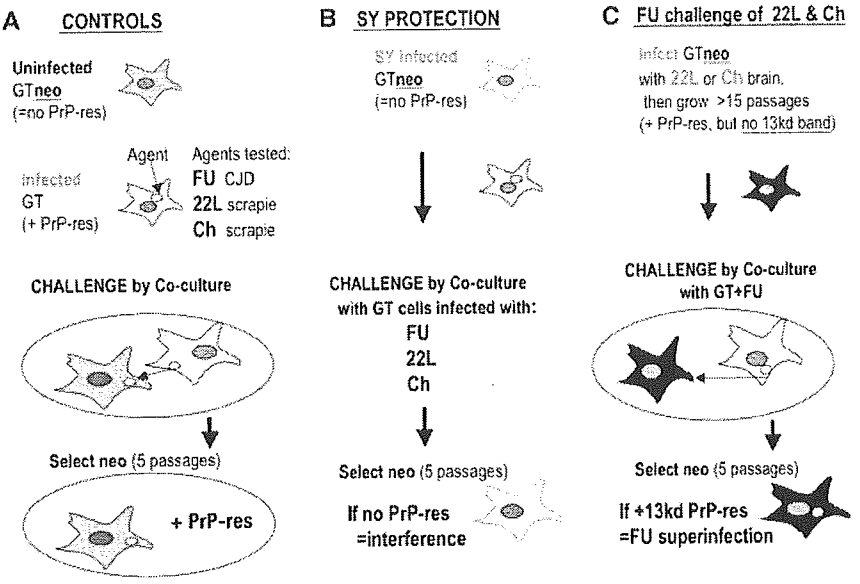

Fig. 1. In vitro interference strategy: Coculture challenges of (A) uninfected control cells, (B) SY-infected cells, and (C) scrapie-infected cells. Target GTneo cells were challenged with mock GT or infected GT cells by coculture for 2 days. GT challenge cells were then killed by G418 treatment, and resistant GTneo cells were analyzed for PrPres (*11*). For FU challenges, GTneo cells were newly infected with 22L or Ch scrapie brain homogenates and passaged >15 times before coculture.

titers, and may not be detectable in all infectious samples [e.g., (*1*, *4*, *12*, *13*)], its presence does indicate infection in GT cells (*10*).

GTneo target cells were exposed to uninfected brain tissue or to equal numbers of uninfected donor cells (i.e., mock-infected as in Fig. 1A). Such control GTneo cells should fail to produce PrPres. In contrast, mock-infected GTneo cells challenged with infected GT cells should become persistently infected and display PrPres long after the GT cells are removed by G418 treatment. Challenges of GTneo cells by GT cells infected with the agents 22L scrapie (GT+22L), Ch scrapie (GT+Ch), or FU-CJD (GT+FU) were rapidly effective (Fig. 2A). A large amount of PrPres was produced by all the control target cells after challenge with infected GT cells, but no PrPres was present after exposure to uninfected brain tissue (in this and in three or more repeat experiments per condition). Further in vitro passages of these GTneo target cells showed stable production of PrPres, indicating persistent infection by each of the challenge agents. Some TSE agents have been associated with variant PrPres band patterns (*14*). The three major PrPres bands were the same in all infected cells. However, an extra, highly reproducible, 13-kD band of PrPres was seen only in FU-infected cells. Antibodies identified this as a C-terminal PrPres fragment (Fig. 2A, C-13). Because this band was not present with any of the other agents, we could use it to specifically diagnose FU superinfection. Moreover, with all challenge agents, rapid infection with de novo production of large amounts of PrPres was apparent by 25 days in culture, whereas intracerebral inoculation with FU homogenates takes more than 90 days to induce brain PrPres (*8*).

In parallel with these controls, we tested whether SY could interfere with FU superinfection in culture as it does in mice, and we also tested whether SY infection could reduce susceptibility to presumably unrelated scrapie agents (Fig. 1B). The neomycin plasmid was added to PrPres-negative but persistently infected SY cells (as verified by repeated bioassays) (*10*, *11*). The lack of PrPres in SY-infected target cells greatly simplified the interference assay. After challenge, a continued lack of PrPres would indicate that covert SY infection protected cells from superinfection. In all these experiments, the number of infectious particles in challenge cells was higher than in target cells by a factor of ≥10,000 (*11*). No PrPres was detected in the GTneo+SY cells challenged with 22L cells (SY/22L lane, Fig. 2B). Thus, SY infection interfered with 22L superinfection. G418 selection also visibly removed all of the abundant PrPres of challenge cells. Persistent SY infection additionally interfered with GT+Ch scrapie agent and GT+FU CJD agent challenges. Only a barely detectable smear of signal was seen in the PrPres gel region (Fig. 2B). Moreover, the 13-kD PrPres band elicited by FU infection was never detectable in the FU-challenged SY cells, and the lack of any distinguishing strain-specific PrPres patterns for the other three common major PrPres bands made it impossible to determine whether the ± signal was due to low levels of the challenge strain. Two repeat experiments reconfirmed that SY interfered with superinfection by 22L, Ch, and FU agents (Table 2). Although the PrPres results do not permit us to conclude that there was complete prevention of superinfection, the interference of SY against 22L, Ch, and FU agents in vitro was manifest, and in marked contrast to the results with unprotected cells.

Because the 13-kD PrPres band was seen only after FU infection (Fig. 2A), it was possible to test whether scrapie agents could protect against the FU-CJD agent (Fig. 1C). We established new persistent infections of GTneo cells by standard application of infected brain homogenates (*9*, *10*), and verified that these newly infected GTneo cells continued to produce substantial amounts of

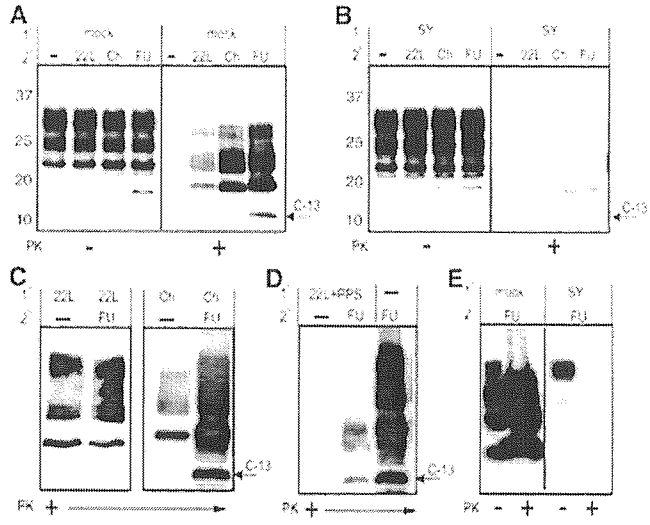

Fig. 2. Immunoblots of control and infected target cells. (A) Challenge of mock-infected and (B) SY-CJD–infected GTneo target cells by coculture with uninfected GT cells (–) or with infected GT+22L, GT+Ch, and GT+FU cells. Primary agent (1°) and challenge agent (2°) are indicated with total PrP compared to PrPres after limited proteinase K (PK) digestion. No PrPres is detectable in SY-infected cells, and the C-13 band is seen only in FU-infected cells. Markers (in kilodaltons) are at left. (C) PrPres after mock (–) and FU-CJD challenge (FU) of 22L scrapie GTneo cells (left) versus challenge of Ch scrapie GTneo cells (right). Mock controls (–) both show high levels of PrPres in scrapie-infected cells before FU challenge. After FU challenge of 22L cells, the pattern and amount of PrPres is unchanged, indicating no appreciable superinfection, and the C-13 band is undetectable. In contrast, massive superinfection by FU is apparent in Ch-infected cells, with markedly increased PrPres and a clear 13-kD band (C-13). (D) Superinfection of "cured" 22L cells treated with pentosan polysulfate (22L+PPS). PrPres is not detectable in the "cured" unchallenged cells (left lane) as compared with the original 22L-infected cells in (C). "Cured" cells challenged with FU became susceptible to FU superinfection and showed the C-13 FU diagnostic band (middle lane, arrow). The "cured" cells, however, showed less PrPres than did the parallel FU-challenged uninfected controls (right lane), possibly suggesting residual 22L scrapie agent. (E) Mock- and SY-infected target cells (minus neo plasmid or G418 selection) challenged with GT+FU cells separated by a 0.4μ filter. Mock cells became infected (positive for PrPres, left), whereas SY-infected cells were protected (right). C-13 is not seen in whole-cell lysates (*11*).

Table 2. Interference results in three replicate experiments. Symbols: +, strong PrPres signal (positive infection); –, no detectable PrPres; ±, barely detectable or questionable PrPres signal between 19 and 30 kD. C-13 is the FU diagnostic band. FU-CJD, 22L, and Ch scrapie infectious challenges were of greater magnitude than in previous in vivo studies (*11*).

Agent		PrPres		Interference
1° first	2° challenge	19 to 30 kD	C-13	
Mock	FU-CJD	+ / + / +	+ / + / +	No
Mock	22L scrapie	+ / + / +	– / – / –	No
Mock	Ch scrapie	+ / + / +	– / – / –	No
SY-CJD	Mock	– / – / –	– / – / –	—
SY-CJD	FU-CJD	± / – / –	– / – / –	Yes
SY-CJD	22L scrapie	– / ± / ±	– / – / –	Yes
SY-CJD	Ch scrapie	± / – / –	– / – / –	Yes
22L scrapie	FU-CJD	+ / + / +	– / – / –	Yes
Ch scrapie	FU-CJD	+ / + / +	+ / + / +	No

pathologic PrPres for >15 in vitro passages before challenging them with GT+FU cells. Both the 22L and Ch scrapie–infected GTneo cells, but not the parallel mock-infected cells, showed large amounts of the three major PrPres bands, but not the extra 13-kD band that was diagnostic for FU infection. These 22L and Ch scrapie–infected GTneo cells were then challenged with FU+GT cells that displayed the 13-kD band (as in Fig. 2A). A large increase in PrPres and/or the appearance of the extra 13-kD PrPres band in scrapie-infected GTneo cells would show that these particular scrapie agents failed to prevent superinfection by FU. Superinfection would also prove that high levels of PrPres are not protective.

The scrapie strains 22L and Ch displayed markedly different capacities for interfering with FU superinfection (Fig. 2C). Target 22L cells were protected against FU superinfection. The PrPres intensity and band patterns of 22L cells exposed to FU (22L/FU lane, Fig. 2C) were the same as in 22L controls (22L/– lane), and the lack of the FU-diagnostic 13-kD PrPres band further confirmed that only the initial 22L infection was present. The 13-kD PrPres band also did not appear with additional in vitro passages, indicating that FU was probably not covertly contaminating the target cells. These results were reproducible (Table 2).

In sharp contrast, Ch scrapie infection did not protect GTneo cells from FU superinfection. PrPres accumulation in these FU-challenged cells (Ch/FU lane, Fig. 2C) was considerably more intense than in mock cells (Ch/– lane), and consistent with the amount of pathologic PrPres that would be provoked by infection with both agents. Additionally, there was a strong 13-kD PrPres signal indicating FU superinfection (Fig. 2C and Table 2). Hence, enormous amounts of PrPres provoked by the Ch agent did not prevent massive superinfection by a second strain. Because in situ studies show that FU infects most GT cells (*10*), it is likely that a fair proportion of the Ch/FU cells were doubly infected. Brain tissue can also be doubly infected, and each agent breeds true despite cocultivation in that tissue for >200 days (*3*). In sum, two scrapie strains eliciting the same PrPres band pattern show markedly different susceptibilities to a CJD agent that provokes an extra PrPres band.

To further show that interference depended on persistent infection, we "cured" GT+22L neo cells by treating them with pentosan polysulfate (*11*) until PrPres was undetectable (Fig. 2D). We then challenged these "cured" 22L cultures and parallel mock controls with GT+FU as above. These "cured" cultures became susceptible to FU superinfection and showed the diagnostic FU 13-kD band (Fig. 2D), unlike the 22L-protected cells (Fig. 2C). This experiment also shows that the 22L agent, rather than some new cellular characteristic induced by neo plasmid/G418 selection, was the ultimate cause of interference.

Direct cell-to-cell contacts may aid agent transmission in vivo, as in the transfer of infectious agent from follicular dendritic cells to transiting white blood cells (*15*). We found that concentrated supernatants from both 22L- and FU-infected GT cells were less infectious than the remaining whole washed cells by a factor of ~1000, as measured by bioassay. We also prevented direct cell-to-cell contact with 0.4μ filters placed between challenge cells and GT+SY target (minus neoplasmid) cells. This would permit the transit of large viruses and aggregates but not whole cells. Equal numbers of healthy challenge and target cells were plated and exposed for 2 days, and the separated target cells were then passaged and analyzed (*11*). Target control cells required ≥8 in vitro passages to produce PrPres and did not always become positive, unlike the cocultures described above. However, despite this caveat, SY infection did interfere with FU superinfection as compared to more typical controls (Fig. 2E). Thus, SY infection rather than neo transformation and G418 selection was the primary cause of interference.

We have shown that infected neural cells in culture carry all the requisite features for

mounting a substantial TSE interference effect. No immune system cells were necessary for this protection, and stable interfering infections were reproducibly achieved without cloning. Interference did not depend on the presence or absence of abnormal PrP. Only persistent infection protected target cells from superinfection. Additionally, only particular agent-strain combinations showed positive interference, and these could not be predicted from cellular PrPres amounts or banding patterns. Moreover, despite continuous replication in cells with PrPres band patterns very different from those found in brain tissue, SY and FU CJD agents each breed true when reinoculated into mice, as does rodent-passaged scrapie reinoculated in sheep (*10*). The stability of the BSE agent also contrasts with the many different PrPres patterns seen in various affected species. Together, these results are not compatible with the common assumption that TSE strains are encoded by some unresolved type of PrPres folding (*16*, *17*). Indeed, there is still no conclusive evidence that any recombinant or amplified form of abnormal PrP can infect normal animals directly, reproduce meaningful levels of infectivity, or encode all the strain differences observed in mice infected with scrapie, CJD, and BSE agents.

Unlike heterogeneous aggregates of pathological PrP, infectious TSE particles have a discrete viral size of ~25 nm and 10^7 daltons (as assessed by field flow fractionation and high-pressure liquid chromatography, respectively) (*18*), and releasing their tightly bound nucleic acids destroys infectivity (*19*). Thus, some TSE agents such as SY may produce defective interfering particles, as found in many persistent viral as well as noncoding human viroid infections (*20*, *21*). Unlike pathologic host PrP, TSE agents can also provoke innate cellular defenses, including intracellular and diffusible factors that are not restricted to immune system cells (*7*, *8*), and such factors are likely to be involved in interference. Small interfering RNAs with extensive secondary structure may also be evoked by TSE agents, and these can provide even greater strain specificity (*22*). Notably, several small RNAs with extensive secondary structure have been identified in TSE-infected but not in normal brain tissue (*23*), and such motifs deserve further study in TSE culture models.

Cocultures were more efficient than mouse bioassays and can be useful for rapid assessment of agent purification and recovery (*24*). Additionally, they may provide a sensitive test for cells that are infected but show no PrPres (such as white blood cells), and they may be useful for evaluating a wide range of evolving TSE agents that have become important epidemiologically, such as those that cause BSE and chronic wasting disease (CWD). The resistance of cells infected with a prototypic sporadic CJD agent (SY) to two scrapie strains supports the suggestion that a commensal but rarely pathogenic TSE agent may help protect people against infection by sheep TSE strains in nature (*4*), and may explain why so few people have developed BSE-linked CJD (*25*). The clustering of sporadic CJD cases is also consistent with an environmental agent of low virulence (*26*).

References and Notes

1. L. Manuelidis, W. Fritch, Y. G. Xi, *Science* **277**, 94 (1997).
2. L. Manuelidis, *Proc. Natl. Acad. Sci. U.S.A.* **95**, 2520 (1998).
3. L. Manuelidis, Z. Y. Lu, *Neurosci. Lett.* **293**, 163 (2000).
4. L. Manuelidis, Z. Y. Lu, *Proc. Natl. Acad. Sci. U.S.A.* **100**, 5360 (2003).
5. A. Dickinson, H. Fraser, V. Meikle, G. Outram, *Nature New Biol.* **237**, 244 (1972).
6. C. Baker, L. Manuelidis, *Proc. Natl. Acad. Sci. U.S.A.* **100**, 675 (2003).
7. C. Baker, Z. Lu, L. Manuelidis, *J. Neurovirol.* **10**, 1 (2004).
8. Z. Lu, C. Baker, L. Manuelidis, *J. Cell. Biochem.* **93**, 644 (2004).
9. N. Nishida *et al.*, *J. Virol.* **74**, 320 (2000).
10. A. Arjona, L. Simarro, F. Islinger, N. Nishida, L. Manuelidis, *Proc. Natl. Acad. Sci. U.S.A.* **101**, 8768 (2004).
11. See supporting data on *Science* Online.
12. C. Lasmezas *et al.*, *Science* **275**, 402 (1997).
13. Y. G. Xi, A. Ingrosso, A. Ladogana, C. Masullo, M. Pocchiari, *Nature* **356**, 598 (1992).
14. A. Hill *et al.*, *Brain* **126**, 1333 (2003).
15. L. Manuelidis *et al.*, *J. Virol.* **74**, 8614 (2000).
16. S. Prusiner, *Proc. Natl. Acad. Sci. U.S.A.* **95**, 13363 (1998).
17. G. S. Jackson, J. Collinge, *Mol. Pathol.* **54**, 393 (2001).
18. T. Sklaviadis, R. Dreyer, L. Manuelidis, *Virus Res.* **3**, 241 (1992).
19. L. Manuelidis, T. Sklaviadis, A. Akowitz, W. Fritch, *Proc. Natl. Acad. Sci. U.S.A.* **92**, 5124 (1995).
20. A. Barrett, *Curr. Top. Microbiol. Immunol.* **128**, 55 (1986).
21. J. Wu *et al.*, *World J. Gastroenterol.* **11**, 1658 (2005).
22. P. M. Waterhouse, M. B. Wang, T. Lough, *Nature* **411**, 834 (2001).
23. L. Manuelidis, in *Transmissible Subacute Spongiform Encephalopathies: Prion Diseases*, L. Court, B. Dodet, Eds. (Elsevier, Paris, 1966), pp. 375–387.
24. L. Manuelidis *et al.*, unpublished data.
25. L. Linsell *et al.*, *Neurology* **63**, 2077 (2004).
26. P. Smith, S. Cousens, J. d'Huillard Aignaux, H. Ward, R. Will, *Curr. Top. Microbiol. Immunol.* **284**, 161 (2004).

27. Supported by NIH grant NS12674, U.S. Department of Defense grant DAMD-17-03-1-0360, and a grant from the Ministry of Health, Labor and Welfare, Japan.

Supporting Online Material
www.sciencemag.org/cgi/content/full/310/5747/493/DC1
Materials and Methods

29 July 2005; accepted 21 September 2005
10.1126/science.1118155

Interlinked Fast and Slow Positive Feedback Loops Drive Reliable Cell Decisions

Onn Brandman,[1,2]* James E. Ferrell Jr.,[1] Rong Li,[2,3,4] Tobias Meyer[1,2]

Positive feedback is a ubiquitous signal transduction motif that allows systems to convert graded inputs into decisive, all-or-none outputs. Here we investigate why the positive feedback switches that regulate polarization of budding yeast, calcium signaling, *Xenopus* oocyte maturation, and various other processes use multiple interlinked loops rather than single positive feedback loops. Mathematical simulations revealed that linking fast and slow positive feedback loops creates a "dual-time" switch that is both rapidly inducible and resistant to noise in the upstream signaling system.

Studies in many biological systems have identified positive feedback as the key regulatory motif in the creation of switches with all-or-none "digital" output characteristics (*1*). Although a single positive feedback loop (*A* activates *B* and *B* activates *A*) or the equivalent double-negative feedback loop (*A* inhibits *B* and *B* inhibits *A*) can, under the proper circumstances, generate a bistable all-or-none switch (*1*–*5*), it is intriguing that many biological systems have not only a single but multiple positive feedback loops (Table 1). Three examples of positive feedback systems are shown in more detail in Fig. 1.

[1]Department of Molecular Pharmacology, Stanford University School of Medicine, Stanford, CA, 94305, USA. [2]Physiology Course 2004, Marine Biological Laboratory, Woods Hole, MA 02543, USA. [3]Department of Cell Biology, Harvard Medical School, Boston, MA 02115, USA. [4]The Stowers Institute for Medical Research, Kansas City, MO 64110, USA.

*To whom correspondence should be addressed. E-mail: onn@stanford.edu

Polarization in budding yeast depends on two positive feedback loops, a rapid loop involving activity cycling of the small guanosine triphosphatase Cdc42 and a slower loop that may involve actin-mediated transport of Cdc42 (Fig. 1A) (*6*). In many cell types, the induction of prolonged Ca^{2+} signals involves initial rapid positive feedback loops centered on Ca^{2+} release mediated by inositol 1,4,5-trisphosphate (IP3) combined with a much slower loop that induces Ca^{2+} influx mediated by the depletion of Ca^{2+} stores (*7*, *8*) (Fig. 1B). *Xenopus* oocytes respond to maturation-inducing stimuli by activating a rapid phosphorylation/dephosphorylation–mediated positive feedback loop (between Cdc2, Myt1, and Cdc25) and a slower translational positive feedback loop [between Cdc2 and the the mitogen-activated protein kinase (MAPK or ERK) cascade, which includes Mos, MEK (MAPK kinase), and p42] (Fig. 1C).

The presence of multiple interlinked positive loops raises the question of the performance

JOURNAL OF VIROLOGY, June 2005, p. 7104–7112 Vol. 79, No. 11
0022-538X/05/$08.00+0 doi:10.1128/JVI.79.11.7104–7112.2005

Biological and Biochemical Characteristics of Prion Strains Conserved in Persistently Infected Cell Cultures

Kazuhiko Arima,[1] Noriyuki Nishida,[1] Suehiro Sakaguchi,[1,3] Kazuto Shigematsu,[2] Ryuichiro Atarashi,[1] Naohiro Yamaguchi,[1] Daisuke Yoshikawa,[1] Jaewoo Yoon,[1] Ken Watanabe,[1] Nobuyuki Kobayashi,[1] Sophie Mouillet-Richard,[4] Sylvain Lehmann,[5] and Shigeru Katamine[1]*

Department of Molecular Microbiology and Immunology,[1] and Department of Pathology 2,[2] Nagasaki University Graduate School of Biomedical Sciences, Sakamoto 1-12-4, Nagasaki 852-8523, Japan; PRESTO, Japan Science and Technology Agency, 4-1-8 Honcho Kawaguchi, Saitama, Japan [3]; Institut André Lwoff, CNRS UPR 1983-BP8, 94801 Villejuif Cedex, France[4]; and Institut de Genetique Humaine, CNRS UPR 1142, 34396 Montpellier Cedex 5, France[5]

Received 16 August 2004/Accepted 18 January 2005

Abnormal prion protein (PrP^{Sc}) plays a central role in the transmission of prion diseases, but the molecular basis of prion strains with distinct biological characteristics remains to be elucidated. We analyzed the characteristics of prion disease by using mice inoculated with the Chandler and Fukuoka-1 strains propagated in a cultured mouse neuronal cell line, GT1-7, which is highly permissive to replication of the infectious agents. Strain-specific biological characteristics, including clinical manifestations, incubation period as related to the infectious unit, and pathological profiles, remained unchanged after passages in the cell cultures. We noted some differences in the biochemical aspects of PrP^{Sc} between brain tissues and GT1-7 cells which were unlikely to affect the strain phenotypes. On the other hand, the proteinase K-resistant PrP core fragments derived from Fukuoka-1-infected tissues and cells were slightly larger than those from Chandler-infected versions. Moreover, Fukuoka-1 infection, but not Chandler infection, gave an extra fragment with a low molecular weight, ~13 kDa, in both brain tissues and GT1-7 cells. This cell culture model persistently infected with different strains will provide a new insight into the understanding of the molecular basis of prion diversity.

Transmissible spongiform encephalopathies (TSEs) are a series of neurodegenerative disorders that include Creutzfeldt-Jakob disease (CJD), Gerstmann-Straussler-Scheinker syndrome (GSS), and fatal familial insomnia in humans and bovine spongiform encephalopathy and scrapie in animals (23, 25). Human TSEs may have infectious, sporadic, or genetic origins, but the brain tissues from affected individuals always possess an infectious agent, termed prion, capable of transmitting the disease to laboratory animals. The protein-only hypothesis proposes that the abnormal isoform of the prion protein (PrP^{Sc}) accumulated via posttranslational modification of the cellular isoform (PrP^{C}) is the sole component of the infectious particle (25). In fact, while the agent is extremely resistant to inactivation by UV and ionizing radiation, protein denaturants can abolish the infectivity, and moreover, no specific genetic materials for infectious agents have been identified. The two PrP isoforms are distinguishable by their biochemical properties. PrP^{C} is readily soluble in nondenaturing detergents and completely digested by proteinase K (PK), whereas PrP^{Sc} is detergent insoluble and resistant to proteolysis except for the N-terminal region comprising ~67 residues. Structural studies have suggested that the former is rich in alpha-helical structures with small β-sheet regions, but the latter has a high β-sheet content. The central role of PrP in the diseases is exemplified by the fact that PrP-null mice are resistant to the disease (6, 27), by the causal linkage of genetic forms of human TSEs with mutation in the PrP gene (25), and by the dependency of the species barriers on the primary PrP sequences (29). The existence of strain variation, however, has challenged the protein-only hypothesis. Individual infectious agents have been shown to maintain their phenotypic characteristics, including the clinical presentation of disease, the length of the incubation period, and the distribution of vacuolar degeneration and PrP^{Sc} deposition in the central nervous system (CNS) during serial transmission between same-species animals. In addition to these biological characteristics, biochemical differences in PrP^{Sc} have been reported. Transmission of two different inherited human prion diseases, fatal familial insomnia and familial CJD, to mice resulted in the accumulation of PrP^{Sc} with PK-resistant core fragments with molecular masses of 19 and 21 kDa, respectively (35). The difference in the size of PK-resistant PrP^{Sc} fragments has been also documented among agents originating from scrapie and mink spongiform encephalopathies (3). The degree of glycosylation is also proposed to be an important signature of some strains. There are two sites of Asn-linked glycosylation at the C-terminal portion, and the degree of glycosylation is thus represented by the ratio of three glycoforms, di-, mono-, and unglycosylated forms. The unique PrP^{Sc} glycoform pattern, in which the diglycosylated form dominates, in animals and patients affected with bovine spongiform encephalopathy and variant CJD, respectively, is distinct from those of other known strains (11) with a few exceptions (32). Because diversity in the size of a PK-resistant PrP core fragment and the degree of its Asn-linked glycosylation were thought to be consequences of differences in the conformation, it has been hypothesized that strain-specific conformations of PrP^{Sc} could determine the strain phenotype.

* Corresponding author. Mailing address: Department of Molecular Microbiology and Immunology, Nagasaki University Graduate School of Biomedical Sciences, Sakamoto 1-12-4, Nagasaki 852-8523, Japan. Phone: 81-95-849-7057. Fax: 81-95-849-7060. E-mail: katamine@net.nagasaki-u.ac.jp.

However, the strain-specific conformation of PrP^{Sc} and, in particular, its causal relationship with strain phenotypes, still remains controversial (13, 21).

Most of the information regarding strains so far available has been obtained from in vivo experiments using mice or hamsters, a system less advantageous for biochemical approaches to the molecular mechanisms of the strains. Neuronal cell culture models are clearly of greater value for such studies. However, only a few cultured cell lines, including PC12 and mouse neuroblastoma-derived N2a, have been shown to be permissive to scrapie agents (7, 26), and the levels of replication in these cell lines are not satisfactory, at least for quantitative detection of infectivity. Some of us previously demonstrated that cultured mouse neuronal cells expressing a high amount of PrP^{C} were highly permissive to replication of various mouse-adapted strains (15, 18). Arjona et al. recently compared two CJD strains using GT1-7 and N2a58 cells (1). The aim of the present study was to confirm the usefulness of the neuronal cell culture models by comparing phenotypes of mice inoculated with two strains, Chandler and Fukuoka-1. We report here that passage through the cell cultures did not change the strain-specific nature of the biological characteristics and discuss the relationship between strain phenotype and biochemical aspects of the PrP.

MATERIALS AND METHODS

Cell cultures. The mouse neuronal cell line GT1-7 (14) was exposed to mouse brain homogenates infected with each prion strain as described previously (15, 16, 18). The cells were cultured in DMEM containing heat-inactivated fetal bovine serum at 10% and penicillin-streptomycin and split every 5 days at a 1:3 ratio. All cultured cells were maintained at 37°C in 5% CO_2 in the biohazard prevention area of the authors' institution.

Mice. ddY mice used in the experiments were fed under specific-pathogen-free conditions. Experiments involving agent inoculation were conducted in the biohazard prevention area (P3) of the Laboratory Animal Center for Biomedical Research of the authors' institution.

Prion strains. The Fukuoka-1 strain (34) was passaged three times in the brains of ddY mice. The brains infected with Chandler strains were kindly donated by B. Caughey and R. Carp, respectively. The pooled brains were homogenized to 1% (wt/vol) in cold phosphate-buffered saline (PBS) containing 5% glucose. Cultured cell lysates were prepared by sonication in PBS. All of the homogenates and cell lysates were kept at −80°C until use.

Determination of LD_{50}. Confluent cell cultures in a 100-mm dish (approximately 7.5×10^6 cells) were sonicated in 0.5 ml of PBS. Before use, the cells were cultured for more than 30 passages following the initial ex vivo challenges. The cultured cell lysates and 1% (wt/vol) homogenates of brain tissues were serially diluted 10-fold with PBS, from 10^0 to 10^{-6}, and 20 μl of each dilution was inoculated into the right brain (five mice for each group). The inoculated mice were observed until 364 days after inoculation. The onset of disease was determined as previously described (28). The 50% lethal dose (LD_{50}) was determined according to the Behrens-Karber formula (10).

Histology. The brains were fixed in 4% paraformaldehyde and sectioned into 7-μm-thick sections at levels 250 and 500, as described by Sidman et al. (30). The tissue sections were stained with hematoxylin and eosin. The pattern of vacuolation was examined in 9 areas, namely the midbrain, hypothalamus, thalamus, hippocampus, paraterminal body, posterior cortex, cerebellar medulla, cerebellar granular layer, and cerebellar molecular layer. The vacuolation score was established based on the pattern, size, and density of the vacuoles using standard criteria from grade 0 for none and grade 5 for maximum vacuolation (9)

Antibodies. The anti-PrP polyclonal mouse antiserum used was described previously (19). The IBL-N rabbit antibody against N-terminal peptides of PrP and M20 goat antibody to C-terminal PrP peptides were purchased from Immuno Biological Laboratories (Gunma, Japan) and Santa-Cruz Biotech (Santa Cruz, CA), respectively. Horseradish peroxidase (HRP)-conjugated anti-mouse and -rabbit immunoglobulin G antibodies were purchased from Amersham. HRP-conjugated anti-goat immunoglobulin G antibodies were purchased from Santa-Cruz Biotech.

Immunoblotting. Confluent cultures were lysed for 30 min at 4°C in Triton-DOC lysis buffer (50 mM Tris-HCl [pH 7.5] containing 150 mM NaCl, 0.5% Triton X-100, 0.5% sodium deoxycholate, and 2 mM EDTA). After 1 min of centrifugation at 500 × *g*, the supernatant was collected and its total protein concentration was measured using the Bio-Rad protein assay. To detect PrP^{Sc}, the brain homogenates and cell lysates, with the protein concentration adjusted to 10 mg/ml, were treated with 100 μg/ml of proteinase K (Sigma) at 37°C for 30 min. To remove N-linked glycosylation, PNGase F was used according to the manufacturer's protocol (New England Biolabs) before PK digestion. The samples were boiled for 5 min in sodium dodecyl sulfate (SDS) loading buffer (50 mM Tris-HCl, pH 6.8, containing 5% glycerol, 1.6% SDS, and 100 mM dithiothreitol) and subjected to SDS–12% polyacrylamide gel electrophoresis. The proteins were transferred onto an Immobilon-P membrane (Millipore) in transfer buffer containing 15% methanol at 400 mA for 60 min, and the membrane was blocked with 5% nonfat dry milk in TBST (10 mM Tris-HCl [pH 7.8], 100 mM NaCl, 0.1% Tween 20) for 1 h at room temperature and reacted with anti-PrP antibodies. Immunoreactive bands were visualized by HRP-conjugated secondary antibodies using an enhanced chemiluminescence system (ECL; Amersham Pharmacia Biotech).

RESULTS

Biological characteristics of prion strains in cultured cells: clinical signs in inoculated mice. To examine the biological characteristics of the Chandler and Fukuoka-1 prion strains, GT1-7 cells independently infected with the two strains as well as infected mouse brain homogenates were inoculated into the brains of ddY mice. As shown in Table 1, all of the homogenates produced neurological symptoms and subsequent death in the inoculated mice. They exhibited some common clinical signs, such as weight loss, ruffled and greasy yellowish hair, tremor, hypersensitivity to sound and touch, and locomotor disturbance. However, all of the Chandler-infected mice were hyperactive at the early stages of the disease, in contrast to the progressive hypoactivity of Fukuoka-1-infected mice. When the mice at the terminal stages were sacrificed, a markedly extended bladder, due to urination disturbance, was observed in Fukuoka-1-inoculated, but not Chandler-inoculated, mice. These strain-specific symptoms were reproduced without exception in all of the mice, irrespective of whether brain homogenates or cultured cell lysates were used.

Incubation periods in inoculated mice. As shown in Table 1, the incubation periods of the mice inoculated with 1% brain homogenates of Fukuoka-1 and Chandler were 128.6 ± 9.9 days (mean ± standard deviation) and 149.8 ± 4.4 days, respectively. Interestingly, GT1-7 cells infected with Fukuoka-1 also exhibited a shorter incubation period than Chandler-infected cells: 139.7 ± 12.5 versus 150.2 ± 5.9 days. To analyze more quantitatively, the brain homogenates and GT1-7 cell lysates infected with Fukuoka-1 and Chandler, designated Fukuoka-1/brain, Chandler/brain, Fukuoka-1/GT1-7, and Chandler/GT1-7, respectively, were subjected to the end-point 10-fold dilution assay (Table 1). According to Behrens and Korber's formula, the infectious titers were estimated to be $10^{8.1}$ and $10^{8.8}$ LD_{50} units/g of the brain tissues and $10^{5.3}$ and $10^{6.5}$ LD_{50} units/10^7 GT1-7 cells infected with Fukuoka-1 and Chandler, respectively. After each dilution was converted to its infectious titer, the relationships between infectious titers and incubation periods in the four materials were analyzed. As shown in Fig. 1, plots of Fukuoka-1/brain and Fukuoka-1/GT1-7 clustered in the same region, and those of Chandler/brain and Chandler/GT1-7 formed another cluster located at the region representing much longer incubation periods. The linear relationships between infectious titers and incubation periods in brain homogenates and cell lysates in-

TABLE 1. Mortality and incubation periods of mice inoculated with prion strains[a]

Tissue or cell type	Fukuoka-1 strain			Chandler strain		
	Dilution	Mortality (no. dead/total)	Incubation period (days ± SD)	Dilution	Mortality (no. dead/total)	Incubation period (days ± SD)
Brain homogenate[b]	10^{-2}	5/5	128.6 ± 9.9	10^{-2}	5/5	149.8 ± 4.7
	10^{-3}	5/5	139.2 ± 8.9	10^{-3}	5/5	155.4 ± 7.1
	10^{-4}	5/5	145.6 ± 11.4	10^{-4}	5/5	183.4 ± 8.0
	10^{-5}	4/5	184.7 ± 25.7	10^{-5}	5/5	193.4 ± 16.8
	10^{-6}	4/5	250.5 ± 57.4	10^{-6}	3/5	204.0 ± 27.7
	10^{-7}	1/5	230.0	10^{-7}	4/5	248.0 ± 37.4
	10^{-8}	0/5		10^{-8}	0/5	
	10^{-9}	ND[d]		10^{-9}	0/5	
GT1-7 cell lysate[c]	10^{-0}	4/4	139.7 ± 12.5	10^{-0}	4/4	150.2 ± 5.9
	10^{-1}	5/5	137.2 ± 12.6	10^{-1}	4/4	167.3 ± 11.8
	10^{-2}	5/5	152.4 ± 10.0	10^{-2}	5/5	174.0 ± 10.5
	10^{-3}	5/5	199.4 ± 58.7	10^{-3}	5/5	193.6 ± 13.7
	10^{-4}	2/5	211.0 ± 4.2	10^{-4}	4/5	205.7 ± 18.5
	10^{-5}	0/5		10^{-5}	2/5	203.5 ± 27.5
	10^{-6}	0/5		10^{-6}	2/5	275.5 ± 71.4
	10^{-7}	0/5		10^{-7}	0/5	

[a] Twenty-microliter aliquots of serial 10-fold dilutions of GT1-7 cell lysates and brain homogenates (10^2, 1% [wt/vol] homogenate) were inoculated into the brain of a mouse. Inoculated cells were passaged 35 times before use.
[b] Infectious titers of the brain tissues infected with Fukuoka-1 and Chandler were $10^{8.1}$ and $10^{8.8}$ LD_{50} units/g tissue, respectively.
[c] Infectious titers of Fukuoka-1 and Chandler-infected GT1-7 cells were $10^{6.3}$ and $10^{6.5}$ LD_{50} units/10^7 cells, respectively.
[d] ND, not defined.

fected with each strain overlapped but were distinct between the strains (Fig. 1).

Pathological findings in inoculated mice. Brain sections including the hippocampus, thalamus, and cerebellum from inoculated mice at the terminal stage were stained with hematoxylin and eosin. As shown in Fig. 2, although spongiform change, neuronal loss, and gliosis are common characteristics of prion diseases, the severity and distribution of histological abnormalities differed between the brain tissues of Fukuoka-1- and Chandler-infected mice. In the Fukuoka-1-infected brains, large empty vacuoles were prominent mainly in the white matter, and a microcystic structure measuring up to 100 μm in diameter was observed in the cerebellar medulla (Fig. 2a and e). The grey matter was also affected in advanced cases, while the cerebellar granular and molecular layers were not damaged. The vacuoles in Chandler strain-infected brains were distributed equally in the grey and white matter. However, the number of vacuoles was fewer, and the size, an average of 27 μm in diameter, was obviously smaller than that of those from Fukuoka-1 strain-infected brains (Fig. 2b and f). In general, histopathological changes were much more severe in Fukuoka-1-infected tissues compared with those infected with the Chandler strain. These strain-specific pathological profiles were reproduced by inoculation of GT1-7 cell lysates infected with either strain (Fig. 2c, d, g, and h). A semiquantitative evaluation of the number and size of vacuoles (vacuolation score) in selected areas of brain tissues confirmed that the lesion profiles were strain specific (Fig. 3).

Biochemical aspects of PrP. Biochemical characteristics of PrP in the noninfected brain tissues and GT1-7 cells were

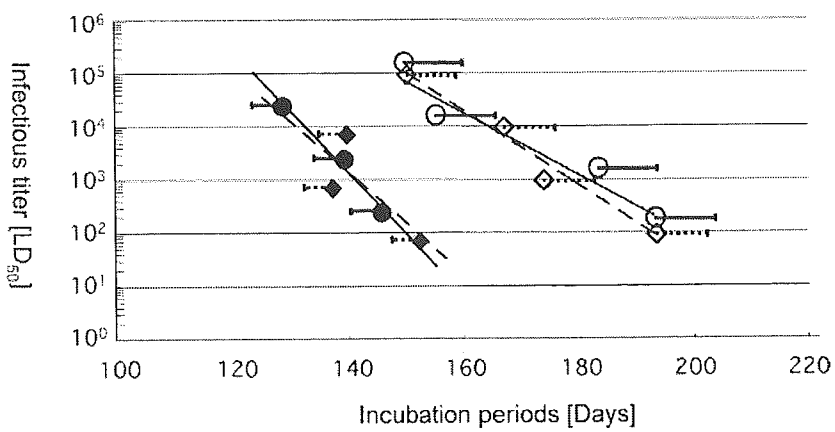

FIG. 1. Linear relationship between infectious titers and incubation periods. Each dilution used in the end-point assay shown in Table 1 was converted to its infectious titer, and the relationships between infectious titers (LD_{50}) and incubation periods (days) in Fukuoka-1/brain (closed circles), Chandler/brain (open circles), Fukuoka-1/GT1-7 (closed squares), and Chandler/GT1-7 (open squares) were analyzed. Horizontal bars indicate standard deviations.

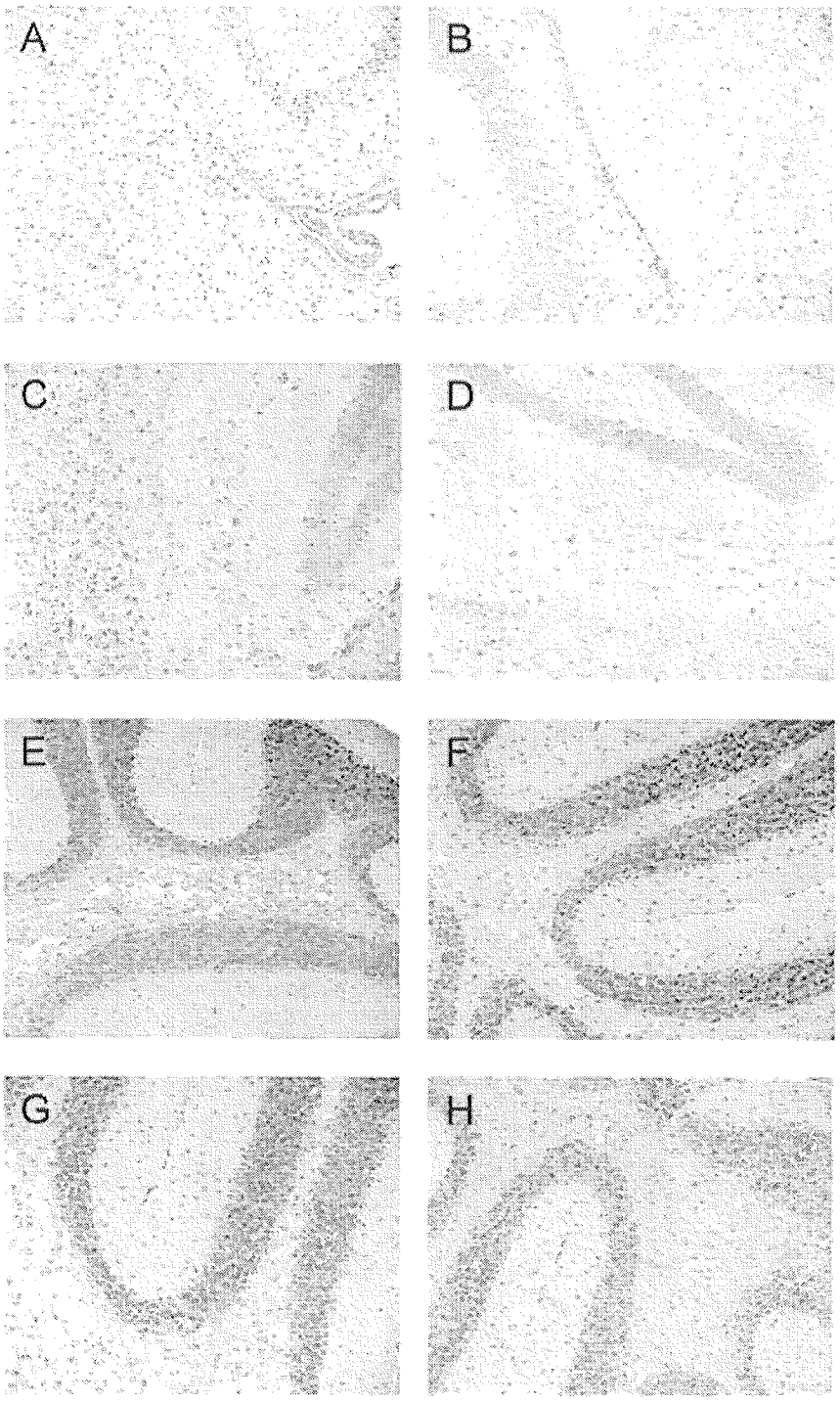

FIG. 2. Histological features of brain tissues infected with prion strains. Sections of the cerebrum (A to D) and cerebellum (E to H) of mice inoculated with Fukuoka-1/brain (A and E), Chandler/brain (B and F), Fukuoka-1/GT1-7 (C and G), and Chandler/GT1-7 (D and H) were stained with hematoxylin and eosin.

compared by immunoblotting. As shown in Fig. 4a, without PK treatment, the IBL-N antibody raised against N-terminal peptides of PrP visualized PrPs both in the noninfected brain and in GT1-7 cells. However, glycosylated components, a diglycosylated band in particular, of the latter migrated much more slowly, indicating that PrP in GT1-7 cells was more heavily glycosylated. Moreover, migration patterns of unglycosylated PrPs from the two sources also looked different: that in GT1-7 cells migrated a little faster. In the tissues and cells infected with Chandler and Fukuoka-1 strains, these host-specific char-

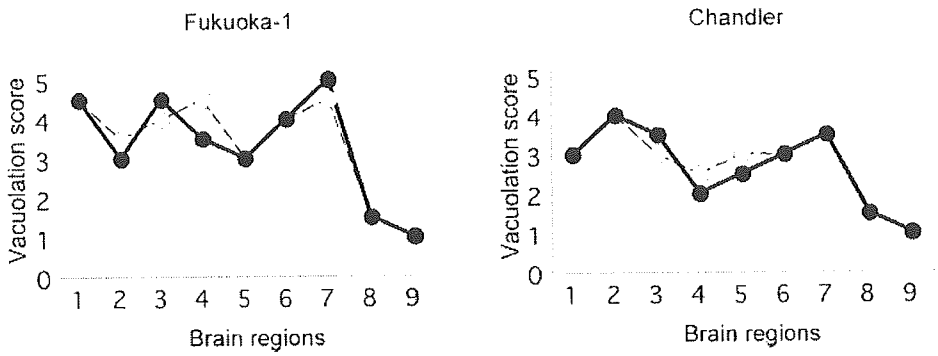

FIG. 3. Region profiles of vacuolation scores in infected mouse brain tissues. Scores were established based on the pattern, size, and density of vacuoles in the tissue using standard criteria with zero for none and five for maximum vacuolation. The pattern of vacuolation was examined in 9 areas, namely the midbrain (1), hypothalamus (2), thalamus (3), hippocampus (4), paraterminal body (5), posterior cortex (6), cerebellar medulla (7), cerebellar granular layer (8), and cerebellar molecular layer (9). Closed and open symbols indicate brain sections infected with brain homogenates and GT1-7 cell lysates, respectively. Each plot indicates the average score of sections from two mice.

acteristics of the PrP structure were essentially preserved. To confirm the difference in the migration patterns between unglycosylated PrPs from brain tissues and GT1-7 cells, Asn-linked glycosylation was completely removed by PNGase F treatment before immunoblotting. As shown in Fig. 4b, regardless of the presence or absence of prion infection, unglycosylated PrP from GT1-7 cells always migrated faster than that from brain tissues.

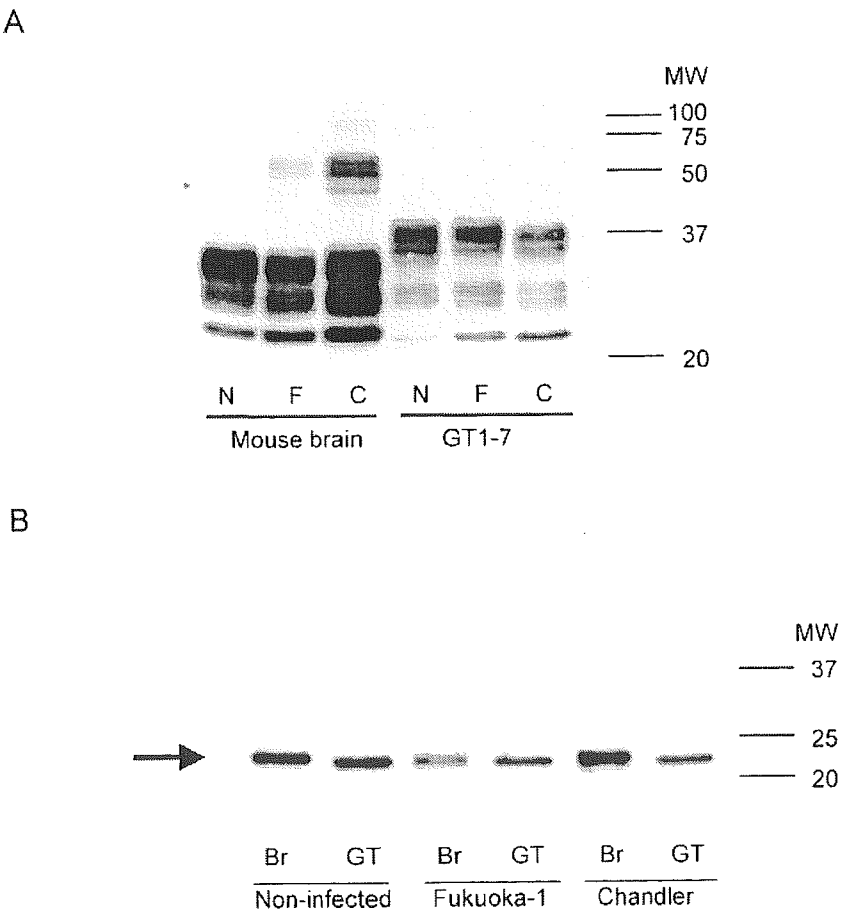

FIG. 4. Detection of PrP in brain homogenates and GT1-7 lysates without PK treatment. (A) Noninfected (N) brain homogenates and GT1-7 cell lysates and those infected with Fukuoka-1 (F) or Chandler (C) prions were subjected to immunoblotting with the IBL-N antibody against N-terminal PrP peptides. (B) The mobilities of nonglycosylated PrPs (arrow) from the brain tissues (Br) and GT1-7 cells (GT) were compared on an immunoblot with the IBL-N antibody after deglycosylation by PNGase F treatment. MW, molecular weight.

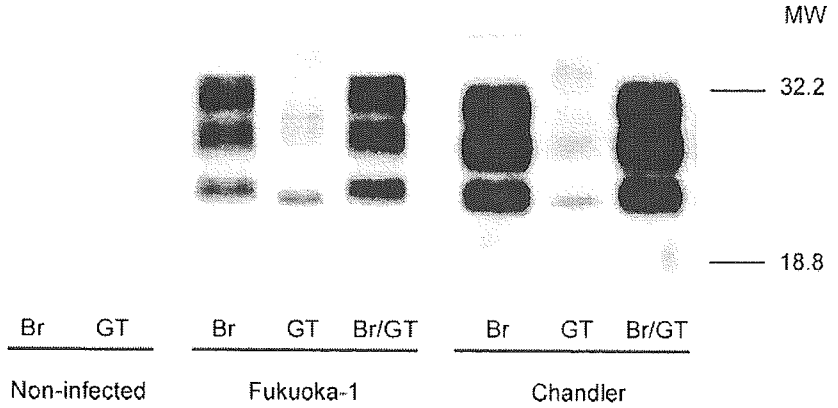

FIG. 5. Immunodetection of PK-resistant PrP in brain homogenates and GT1-7 lysates infected with prion strains. After treatment with PK, noninfected brain homogenates (Br) and GT1-7 cell lysates (GT) and those infected with Fukuoka-1 or Chandler prions were subjected to immunoblotting with polyclonal mouse antisera against PrP. The brain homogenates from terminal-stage mice inoculated with the lysates of GT1-7 cells infected with Fukuoka-1 or Chandler prions (Br/GT) were also analyzed. MW, molecular weight.

Strain-dependent differences in the biochemical aspects of PrP^{Sc}. PK completely digested PrP in the noninfected tissues and cells, while the resistant components (PrP^{Sc}) in the infected tissues and cells were visualized by polyclonal antiserum raised against a recombinant PrP (Fig. 5). Again, diglycosylated PrP^{Sc} in GT1-7 cells migrated to a much higher molecular mass, and its unglycosylated component migrated faster than PrP^{Sc} in the brain tissues. Of importance, PrP^{Sc} developed in the brain tissues of mice inoculated with the infected GT1-7 cell lysates had migration patterns that were indistinguishable from those of PrP^{Sc} in the original brain tissues. PNGase F treatment confirmed the different migration pat-

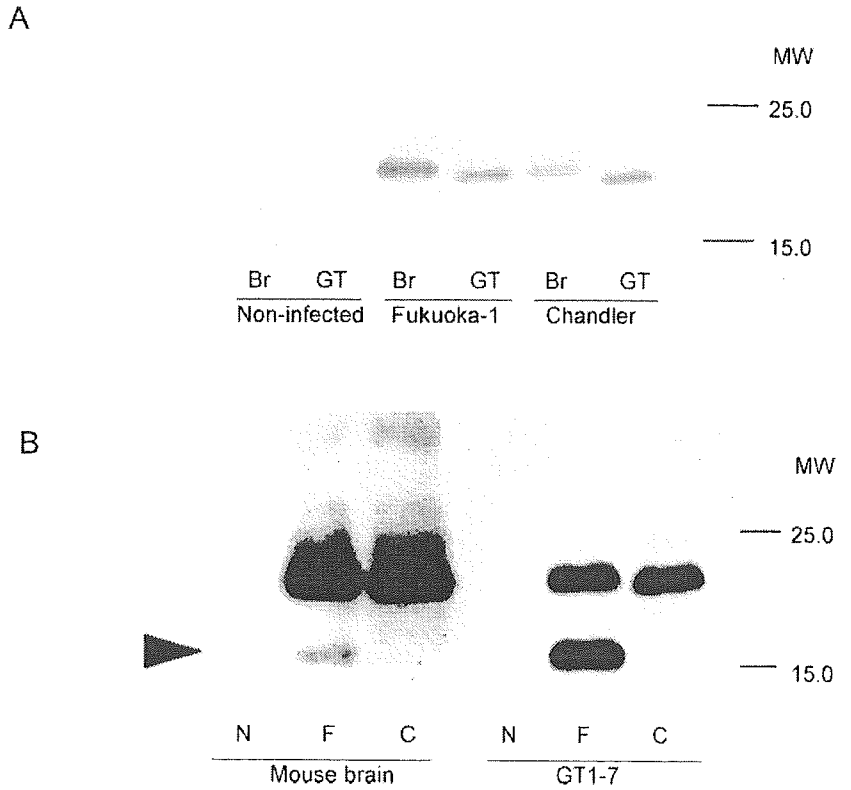

FIG. 6. Differences in the mobility of PK-resistant PrP between hosts and between strains. (A) After successive treatments with PK and PNGase F, mobilities in a gel of nonglycosylated PrP^{Sc} from the brain tissues (Br) and GT1-7 cells (GT) were compared on an immunoblot with the M20 antibody against C-terminal PrP peptides. (B) Mobilities of nonglycosylated PrP^{Sc} generated by Fukuoka-1 (F) and Chandler (C) strains are directly compared by immunoblotting with the M20 antibody. PrP in noninfected tissues and cells (N) is completely digested by PK. The arrowhead indicates the 13-kDa PrP fragment specifically found in the Fukuoka-1-infected tissues and cells. MW, molecular weight.

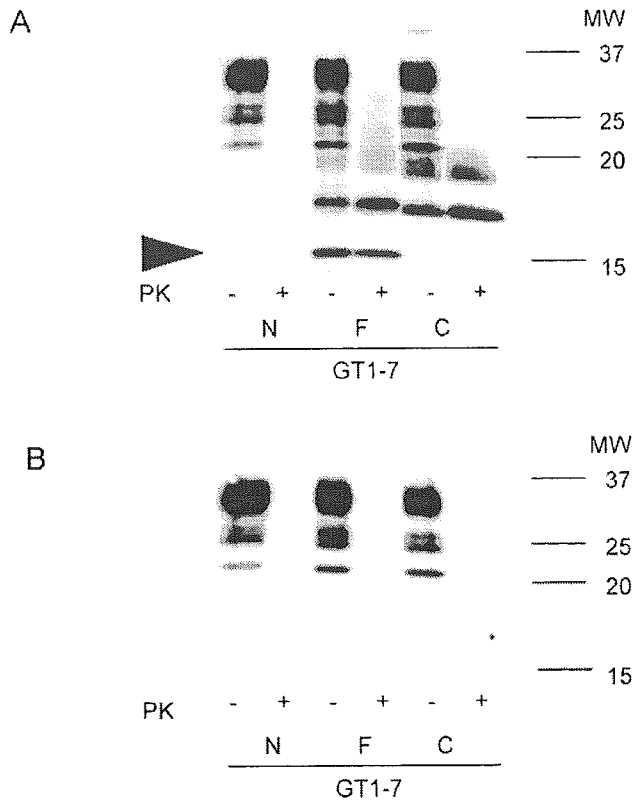

FIG. 7. The 13-kDa PrP fragment is detectable in Fukuoka-1-infected GT1-7 cells even without PK treatment. The cell lysates from noninfected (N) GT1-7 cells and those infected with the Fukuoka-1 (F) or Chandler (C) strain, with (+) or without (−) PK treatment, were subjected to immunoblotting using M20 (A) or IBL-N (B) anti-PrP antibodies. MW, molecular weight.

terns of unglycosylated PrP^{Sc} between the hosts (Fig. 6a). On the other hand, when migration patterns of PrP^{Sc} were directly compared between the strains in the same host on an immunoblot, Fukuoka-1-derived unglycosylated PrP^{Sc} clearly migrated more slowly than the Chandler-derived version (Fig. 6b). These findings strongly suggested that both host-specific and strain-specific factors are involved in the determination of the mobility of PK-resistant unglycosylated PrP^{Sc} in gel. Interestingly, in this immunoblotting, the M20 anti-C-terminal PrP antibody clearly visualized at a low molecular size, ~13 kDa, a component of PrP^{Sc} in Fukuoka-1-infected, but not Chandler-infected, GT1-7 cells (Fig. 5b). A faint but significant band of the 13-kDa fragments was also detectable in the Fukuoka-1-infected brain tissue. Since this fragment was similarly detectable even before the PK treatment and recognized by C-terminal (M20) but not N-terminal (IBL-N) PrP antibodies (Fig. 7), it is likely to be a C-terminal PrP fragment lacking a PK cleavage site.

DISCUSSION

Passage through the neuronal cell cultures of two prion strains, Chandler and Fukuoka-1, did not affect the biological characteristics, including clinical signs, incubation periods, and pathological findings, in the inoculated mice. Carryovers of the original strains into the cultures were unlikely, since the infected cells were cultured for more than 30 passages since the initial ex vivo challenges, assuming that residuals of original brain homogenates in the cultures would be diluted far greater than 10 orders of magnitude. We used a mouse neuronal cell line, GT1-7, which expresses a large amount of PrP^{C} and is highly permissive for replication of the agent (15, 18). Infected GT1-7 cells persistently produced PrP^{Sc} for more than 30 passages without subcloning and maintained high infectious titers of Fukuoka-1 and Chandler at the levels of $10^{5.3}$ and $10^{6.5}$ LD_{50} units/10^{7} cells, respectively. The high degree of competence in prion replication allowed us to quantify infectious titers in the cultured cells by end-point assay. Although data are not shown, we have found that the biological characteristics of the two strains, including clinical signs and incubation periods in the inoculated mice, are also conserved in other two neuronal cell lines, N2a58 (18) and 1C11 (17), which are permissive to various prion strains (16, 18; N. Nishida, unpublished). These findings are consistent with those of previous reports indicating that strain phenotypes did not change during several passages in cultured cells (1, 5).

Western blotting identified some differences in the biochemical features of PrP^{Sc} between the brain tissue and GT1-7 cells. The degrees of glycosylation of PrP^{Sc} derived from the two strains in GT1-7 cells were clearly higher than those in the brain tissues. A similar difference was observed before PK treatment even between the noninfected cells and tissues, suggesting the involvement of host cell factors rather than the strains. In some conditions, the degree of glycosylation (a ratio of glycoforms) of PrP^{Sc} is an important signature of the prion strain (5, 8). However, in our experimental models, it is largely determined by the hosts, presumably due to differences in the enzymatic activities involved in glycosylation or the trafficking pathway of de novo-synthesized PrP^{C}. Host cell- or tissue-determined PrP^{Sc} glycoforms have also been reported by others (31, 36). The mobility of unglycosylated PrP^{Sc} fragments in gel was also distinguishable between the brain tissues and GT1-7. This possibly reflected PK cleavage site heterogeneities due to the difference in the conformation of PrP^{Sc} or an artifact of experimental conditions such as pH (20). However, it is noteworthy that the size difference was also the case for PrP without PK treatment even between the noninfected tissues and cells, arguing against a difference in the PK cleavage sites. Sequencing of PrP cDNAs amplified by reverse transcription-PCR from the brain tissues and GT1-7 cells confirmed that their primary structures were identical (data not shown). A previous study identified, by use of mass spectrometry, six different glycosylphosphatidylinositol (GPI) glycoforms with molecular masses ranging from 2,670 to 3,285 Da in PrP^{Sc} purified from infected hamster brains as well as partially purified PrP^{C} (33). The presence of tissue-specific differences in the GPI composition was also suggested (12). Although the involvement of some difference in the PrP conformation preserved even in a denatured condition cannot be ruled out, a more likely explanation is that it is due to heterogeneity in the composition of GPI moieties. Precise mechanisms for the diversity in PrP structures among the hosts await elucidation, but these structural features are unlikely to affect the strain phenotype, which is shared by the hosts.

It has been hypothesized that the strain-specific conformation of PrP^{Sc} determines the pathological features and func-

tions as a template during pathogenic structural conversion of PrP^{C} to PrP^{Sc} in affected brain tissues (25). The present study also revealed evidence that some strain-specific features of the PrP^{Sc} band pattern on an immunoblot were conserved in the cultured cells. The unglycosylated PK-resistant PrP^{Sc} fragment derived from Fukuoka-1 always migrated more slowly than the Chandler-derived version accumulating in the same host, either in brain tissues or GT1-7 cells. So far, many prion strains, including those of human, sheep, and mink origin, have been characterized by the size of the PrP^{Sc} core fragment generated by PK (2–4, 24). In most cases, the size difference due to the diverse cleavage sites of PK is presumed to be a consequence of the extent of the β-sheet structure. However, Arjona et al. reported that identical PrP^{Sc} band patterns could be observed in GT1-7 cells infected with distinct CJD strains, FU and SY, but were different from those in brain tissues and N2a cells (1). This indicated that the conformational divergence of PrP^{SC} does not necessarily alter strain characteristics. We also demonstrated host-determined divergence, such as glycosylation patterns, which did not affect the biological characteristics of prion strains. Furthermore, the possible involvement of a putative agent or agent-induced factors other than the PrP^{Sc} conformation itself is not precluded. It would be of value to search for such factors that affect the mobility of PrP^{Sc} core fragment by using the cell culture model.

Strikingly, the small 13-kDa PrP^{Sc} fragment detected in Fukuoka-1-infected tissues and cells was not seen in Chandler-infected materials. It is likely that the 13-kDa. Fragment is strain-specific, since Fukuoka-1 but not Chandler resulted in the band not only in GT1-7 cells but also in N2a58 and 1C11 cells (N. Nishida, unpublished). It was PK resistant but detectable before PK treatment, suggesting a lack of PK cleavage sites and the involvement of endogenous proteolytic processes. It is possible that certain environmental factors, for instance, pH and metal ion concentration, influenced by the strain might alter the catalytic activities, but it is also possible that the Fukuoka-1-specific PrP^{Sc} conformation could allow endogenous proteases to access and catalyze the full-length PrP^{Sc}. Although both the Chandler and Fukuoka-1 strains are mouse-adapted ones, the former is of scrapie origin and the latter was derived from a GSS patient carrying the P102L mutation. One group previously demonstrated a similar 13-kDa fragment in the brain tissues from five of seven P102L GSS patients, and this fragment was immunoreactive to a C-terminal PrP antibody but not to 3F4 monoclonal antibody, indicating that it was N-terminally truncated beyond residue 112 (22). It would be intriguing to see whether the specific PrP^{Sc} conformation determined by a particular genetic mutation in the human brain tissues has been conserved during successive transmission to mouse brains and cultured cells lacking such a mutation. Some other reports demonstrated that PrP^{Sc} derived from F198S GSS and CJD also displayed patterns of endogenous proteolysis characteristic of each disorder, leading to distinct sets of PrP^{Sc} fragments (12). It is conceivable that different PrP^{Sc} fragments may exhibit unique biological and pathological consequences in the CNS. The most important pathological consequence of prion strains is the difference in the distribution of vacuolar degeneration among the CNS regions of affected animals. A possible explanation is that each prion strain possesses its own cell tropism. The investigation of cell tropism requires the stable infection of a single cell type which is permissive to more than one strain. In our preliminary experiments using the cell culture models, some strains revealed differential tropism among the cell types examined (N. Nishida, unpublished).

In conclusion, we demonstrated here that the prion strains tested conserved their biological characteristics following cell culture, and the accumulated PrP^{Sc} reproduced some specific features of its band pattern on an immunoblot. However, the molecular basis for conformational divergence of PrP^{Sc} is still enigmatic, and whether or not there is a causal relationship between the PrP^{Sc} conformation and strain phenotype remains to be concluded. Our cell culture models allow the analysis of trafficking and metabolism of PrP, i.e., posttranslational cleavage, glycosylation, recycling, and degradation, etc., which will provide a new insight into the understanding of the molecular basis of prion strains.

ACKNOWLEDGMENTS

We are grateful to Nobuhiko Okimura and Amanda Nishida for technical support and help in manuscript preparation, respectively.

R.A. is a research resident of a 21st Century Center of Excellence (COE) program of Japan. This work was supported by grants from the Ministry of Education, Culture, Sports, Science, and Technology, Japan, and the Ministry of Health, Labor, and Welfare, Japan.

REFERENCES

1. **Arjona, A., L. Simarro, F. Islinger, N. Nishida, and L. Manuelidis.** 2004. Two Creutzfeldt-Jakob disease agents reproduce prion protein-independent identities in cell cultures. Proc. Natl. Acad. Sci. USA **101**:8768–8773.
2. **Baron, T. G., and A. G. Biacabe.** 2001. Molecular analysis of the abnormal prion protein during coinfection of mice by bovine spongiform encephalopathy and a scrapie agent. J. Virol. **75**:107–114.
3. **Bartz, J. C., R. A. Bessen, D. McKenzie, R. F. Marsh, and J. M. Aiken.** 2000. Adaptation and selection of prion protein strain conformations following interspecies transmission of transmissible mink encephalopathy. J. Virol. **74**: 5542–5547.
4. **Bessen, R. A., and R. F. Marsh.** 1992. Biochemical and physical properties of the prion protein from two strains of the transmissible mink encephalopathy agent. J. Virol. **66**:2096–2101.
5. **Birkett, C. R., R. M. Hennion, D. A. Bembridge, M. C. Clarke, A. Chree, M. E. Bruce, and C. J. Bostock.** 2001. Scrapie strains maintain biological phenotypes on propagation in a cell line in culture. EMBO J. **20**:3351–3358.
6. **Bueler, H., A. Aguzzi, A. Sailer, R. A. Greiner, P. Autenried, M. Aguet, and C. Weissmann.** 1993. Mice devoid of PrP are resistant to scrapie. Cell **73**: 1339–1347.
7. **Butler, D. A., M. R. Scott, J. M. Bockman, D. R. Borchelt, A. Taraboulos, K. K. Hsiao, D. T. Kingsbury, and S. B. Prusiner.** 1988. Scrapie-infected murine neuroblastoma cells produce protease-resistant prion proteins. J. Virol. **62**:1558–1564.
8. **Collinge, J., K. C. Sidle, J. Meads, J. Ironside, and A. F. Hill.** 1996. Molecular analysis of prion strain variation and the aetiology of 'new variant' CJD. Nature **383**:685–690.
9. **Fraser, H., and A. G. Dickinson.** 1973. Scrapie in mice. Agent-strain differences in the distribution and intensity of grey matter vacuolation. J. Comp. Pathol. **83**:29–40.
10. **Gilles, H. J.** 1974. Calculation of the index of acute toxicity by the method of linear regression. Comparison with the method of "Karber and Behrens." Eur. J. Toxicol. Environ. Hyg. **7**:77–84.
11. **Hill, A. F., M. Desbruslais, S. Joiner, K. C. Sidle, I. Gowland, J. Collinge, L. J. Doey, and P. Lantos.** 1997. The same prion strain causes vCJD and BSE. Nature **389**:448–450, 526.
12. **Jimenez-Huete, A., P. M. Lievens, R. Vidal, P. Piccardo, B. Ghetti, F. Tagliavini, B. Frangione, and F. Prelli.** 1998. Endogenous proteolytic cleavage of normal and disease-associated isoforms of the human prion protein in neural and non-neural tissues. Am. J. Pathol. **153**:1561–1572.
13. **Manuelidis, L.** 2003. Transmissible encephalopathies: speculations and realities. Viral Immunol. **16**:123–139.
14. **Mellon, P. L., J. J. Windle, P. C. Goldsmith, C. A. Padula, J. L. Roberts, and R. I. Weiner.** 1990. Immortalization of hypothalamic GnRH neurons by genetically targeted tumorigenesis. Neuron **5**:1–10.
15. **Milhavet, O., H. E. McMahon, W. Rachidi, N. Nishida, S. Katamine, A. Mange, M. Arlotto, D. Casanova, J. Riondel, A. Favier, and S. Lehmann.** 2000. Prion infection impairs the cellular response to oxidative stress. Proc. Natl. Acad. Sci. USA **97**:13937–13942.